Evaluation of the Structure of Levee Transitions on Wave Run-Up and Overtopping by Physical Modeling

Drake Oaks[1]; Billy Edge, Dist.M.ASCE[2]; and Patrick Lynett, M.ASCE[3]

Abstract: Coastal regions are continually plagued by high water levels induced by river flooding or hurricane-induced storm surge. As with any protective structure, it is essential to understand potential problematic locations that could result in structural failure and devastating loss. Common coastal protective systems are composed of floodwalls and levees, for each of which practiced methodologies have been used to estimate their performance under design conditions. Methodologies concerning spatial variability are limited, however, and transitions where earthen levees merge with floodwalls are considered areas vulnerable to erosion and possible breaching. Physical modeling of a levee transition is undertaken in a three-dimensional wave basin to evaluate this hypothesis, and the detailed results of this assessment are presented in this paper. From the physical model testing, analysis of the data reveals that overtopping rates tend to be larger immediately near the transition than away from it. The run-up values and floodwall wave heights tend to show potential problematic areas and mimic the variation of overtopping along the levee transition. Under the design conditions tested, extreme overtopping conditions and associated water level values indicate that for the structure to sustain the hydraulic conditions, it must be well armored. It is shown that the variation of the still water level plays the largest role in the magnitude of the measured values, and increasing the peak wave period and wave heights also yields greater overtopping and water levels at the structure. This study highlights the need to understand specific spatial variability along coastal protective systems, and provides a better understanding of the mechanisms affecting overtopping for the specific structure tested. **DOI: 10.1061/(ASCE)WW.1943-5460.0000103.** © *2012 American Society of Civil Engineers.*

CE Database subject headings: Levees; Dikes; Floods; Wave overtopping; Coastal environment.

Author keywords: Levee; Floodwall; Overtopping; Physical model.

Introduction

Throughout many coasts and low-lying areas globally, periodical floods and storm surges cause significant and catastrophic damage. For regions plagued by these incidents of drastic water level increases, a common first and ultimate line of defense is levees and floodwalls. Levees and floodwalls offer sufficient protection against high rises in water level and can protect large areas from inundation; however, the levee and floodwall system is only as durable as its most tenuous area. One such area, highlighted by this research, occurs where an earthen levee transitions into a floodwall with an incorporated levee, referred to in this paper as a levee transition.

Ultimately, the most significant consequence of hydraulic loading that jeopardizes the structural integrity of levees and floodwalls is erosion. The two most common mechanisms that provoke erosion are wave run-up and overtopping. Since the 1953 inundation in the Netherlands, physical modeling of dikes has been conducted to better understand the mechanisms of run-up and overtopping, and it has been refined into a sophisticated method producing accurate estimations beneficial to final designs (Schüttrumpf and van Gent 2003). These models further serve to validate or disprove design guidelines and calibrate numerical models to ensure efficiency and integrity in the final design. More recent events, such as Hurricane Katrina in 2005, have begun to spark even more interest in the evaluation of these coastal protective structures. Hurricane Katrina caused 200 miles of damage to the floodwalls and levees, which is more than 60% of the total Hurricane Protection System (HPS), encompassing the City of New Orleans (Link 2009). Of the 50 breaches in the HPS caused by Hurricane Katrina, all but 4 were induced by overtopping and run-up (Hughes 2008; Nicholson 2007; Sills et al. 2008). The majority of design guidelines used to predict wave overtopping and run-up are purely empirical (Pullen et al. 2007; Technical Advisory Committee for Flood Defence in the Netherlands (TAW) 2002; van der Meer and Janssen 1995) and take into account various parameters that detail the levee geometry and associated hydraulic conditions (Schüttrumpf and van Gent 2003). However, there are many assumptions inherent within the empirical design formulas. Overall, it is important to understand and evaluate the degree of accuracy of the estimations provided by the empirical design guidelines.

Scope of Work

The geometry of the structure under evaluation is closely associated with typical levee and floodwall geometry found in the HPS. The research and the experiments discussed in this paper focus on wave-only overtopping and run-up.

[1]Graduate Research Assistant, Ocean Engineering Program, Texas A&M Univ., College Station, TX 77843. E-mail: drakeoaks@gmail.com

[2]Professor, Sustainable Coastal Processes and Engineering Program, North Carolina State Univ., Raleigh, NC 27695. E-mail: bledge@ncsu.edu

[3]Associate Professor, Ocean Engineering Program, Texas A&M Univ., College Station, TX 77843 (corresponding author). E-mail: plynett@tamu.edu

Note. This manuscript was submitted on November 18, 2010; approved on May 2, 2011; published online on December 15, 2011. Discussion period open until June 1, 2012; separate discussions must be submitted for individual papers. This paper is part of the ***Journal of Waterway, Port, Coastal, and Ocean Engineering***, Vol. 138, No. 1, January 1, 2012. ©ASCE, ISSN 0733-950X/2012/1-53–62/$25.00.

J. Waterway, Port, Coastal, Ocean Eng. 2012.138:53-62.

The basic objectives of this research are as follows:

- Conduct laboratory investigation of levee transition in three-dimensional shallow water wave basin,
- Analyze the resulting data and identify potential problem areas within structure,
- Provide comparison of experimental overtopping measurements with typical empirical design formulas, and
- Develop relationships between hydraulic conditions and observed overtopping for the specific structure tested.

Levee Transition

As mentioned, the levee transition referred to in this paper is the transition between an earthen levee and a vertical floodwall. Fig. 1 provides a generalized picture. The established dimensions of the two sections are addressed in Fig. 2. In the figures, the vertical datum of both sections is at the toe of the levee, which is +0.0 m. The levee section is a composite sloped levee with a 1V:10H berm and a levee crest elevation of 8.23 m. The floodwall section consists of an internal floodwall embedded within an incorporated levee.

The incorporated levee acts as a 1V:10H berm, which dissipates some of the wave energy before encountering the 9.14-m-high floodwall. The backside, or protected side, of the levee section typically integrates a berm in addition to the 1V:3H slope, but is modified in this case to optimize placement within the laboratory, as subsequently discussed. To form the transition, the levee section is rounded at the end to form a levee head. The floodwall section is then placed against the levee section forming the contours at the transition, as illustrated in the three-dimensional rendering in Fig. 3.

Hydraulic Conditions

The testing parameters used for evaluation of the levee transition are given in Table 1, and are approximately representative of design-level conditions along the HPS of New Orleans. Eight tests are conducted with variations in the still water level (SWL), significant wave height (H_s), and peak period (T_p). Note that the significant wave heights provided are the target heights, and will be matched with a spectral H_{mo}. The characteristic values

Fig. 1. Example levee transition (image Google Maps, ©2011)

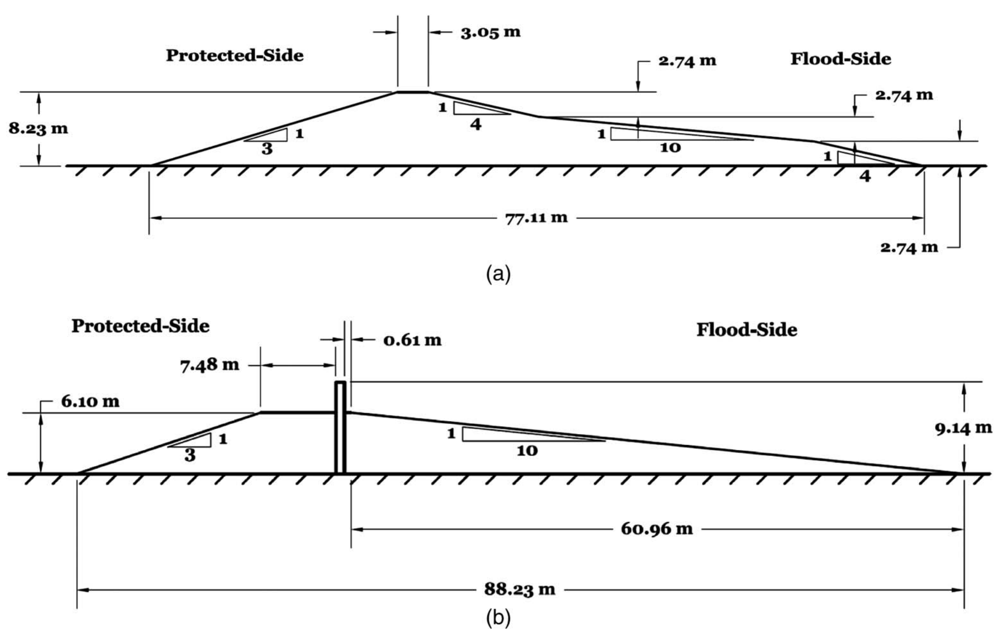

Fig. 2. Cross-sectional prototype dimensions of (top) levee section and (bottom) floodwall section

J. Waterway, Port, Coastal, Ocean Eng. 2012.138:53-62.

Table 1. Prototype Hydraulic Conditions

Test No.	SWL (m)	H_s (m)	T_p (S)
1	5.79	2.29	6
2	5.79	2.29	7
3	5.79	2.29	8
4	5.79	2.29	9
5	6.89	2.74	6
6	6.89	2.74	7
7	6.89	2.74	8
8	6.89	2.74	9

listed in the table serve to formulate a target unidirectional Texel/Marsen/Arsloe (TMA) wave spectrum, which is to be produced by the wave generator in the testing facility. To provide an averaged result and a measure of the experimental scatter in the resulting measured data, three 10-min runs per test are completed, yielding 24 tests in total. All waves are propagated normal to the levee structure. All SWLs are referenced to the originally established datum of the levee toe. The significant wave heights are referenced to the SWL.

Design Guidelines

As mentioned, one objective is to compare the experimental results with typical design formulas. The typical design formulas presented as a comparison are overtopping calculations provided in the European overtopping manual (Pullen et al. 2007) and the TAW manual (2002), as originally defined by van der Meer and Janssen (1995). The Iribarren number, or surf similarity parameter, is calculated as

$$\xi_{\mathrm{op}} = \frac{\tan \alpha}{\sqrt{H_s/L_{\mathrm{op}}}} \tag{1}$$

where α is the flood-side slope of the structure, H_s is the offshore significant wave height (defined as the average of the highest one-third waves), and L_{op} is the offshore wavelength dependent on the peak wave period through

$$L_{\mathrm{op}} = \frac{gT_{\mathrm{p}}^2}{2\pi} \tag{2}$$

where g is gravitational acceleration, and T_{p} is the peak wave period. Pullen et al. (2007) provide guidance for calculation of the deep water wavelength using the mean wave period, T_{m}, in which $T_{\mathrm{p}} = 1.1T_{\mathrm{m}}$. The overtopping calculations in this paper are based on the use of T_{m}, requiring use of the ratio

$$\frac{q}{\sqrt{gH_{mo}^3}} = \frac{0.067}{\sqrt{\tan \alpha}} \gamma_b \xi_{op} \exp\left(-4.3 \frac{R_c}{H_{mo}} \frac{1}{\xi_{op}\gamma_b\gamma_f\gamma_\beta\gamma_v}\right) \tag{3}$$

with a maximum of

$$\frac{q}{\sqrt{gH_{\mathrm{mo}}^3}} = 0.2 \exp\left(-2.3 \frac{R_{\mathrm{c}}}{H_{\mathrm{mo}}} \frac{1}{\gamma_{\mathrm{f}}\gamma_\beta}\right) \tag{4}$$

where q = average wave overtopping discharge (e.g., m^3/m); H_{mo} = spectral significant wave height at the toe of the levee; γ_{f} = reduction factor for slope roughness; γ_β = reduction factor for oblique wave attack; γ_{b} = reduction factor for a berm; γ_{v} = reduction factor for a vertical wall on the slope; and R_{c} = free crest height above the SWL. The free crest, or freeboard, is the vertical distance between the SWL and the crest of the levee or dike.

These traditional empirical equations [Eqs. (1)–(4)] are applied to specific cross sections of levees or floodwalls under specific wave conditions, indirectly assuming that the cross sections are uniform for a given levee or floodwall span; in other words, the equations do not provide any temporal or spatial variability. Clearly, the structure under scrutiny does not satisfy the assumption of cross-sectional uniformity.

Testing Environment

All testing was conducted at the Reta and Bill Haynes ’46 Coastal Engineering Laboratory at Texas A&M University, College Station, Texas. A shallow water wave basin is contained within the laboratory and has the following dimensions: length of 36.6 m, width of 22.9 m, and water depth up to 1.22 m. The basin houses a directional wave basin that operates to a depth of 1 m, creating waves up to 61 cm. The piston-type wave generator is composed of 48 independent paddles, enabling wave directionality and the generation of multiple spectral models. The waves are generated from the wave generator and propagate over a flat bottom until interaction with the tested structure. Waves that transmit beyond the structure encounter a rock beach, which dissipates approximately 85% of the wave energy.

Of course, laboratory effects potentially influence measurements during testing. The largest model effect was generated by the sudden drop-off at the model sides. This sudden drop-off caused the wave crests to refract toward the levee, resulting in abnormally large overtopping rates near the end of the levee section and floodwall section. Consequently, overtopping measurements and floodwall wave gauge measurements recorded near the levee end and floodwall end are not represented. Additionally, seiching within the basin was limited by additional wave absorbers at the sidewalls.

Experimental Setup and Physical Modeling Process

Levee Transition Model

As noted earlier, the levee transition consists mostly of two parts, the floodwall section and the levee section. Fig. 3 illustrates the transition between these two sections. The levee section, highlighted in green, is rounded at the transition as it intersects with the floodwall section, which is presented in white. The model is composed of a rock core with additional wooden supports within. Model scaling is 1:20 using Froude similitude. On top of the rock core, a 10-cm concrete shell is placed to provide a smooth surface and enable accurate representation of the detailed contours present on the flood side of the model, especially at the transition. The floodwall is composed of a wooden frame with sheet metal on either side. The floodwall is built within the incorporated levee, as shown in Fig. 2, to allay any movement of the wall during testing. The 1:20 scale yields a model that is approximately 10.7 m long and 4.4 m wide with a floodwall crest elevation of 45.72 cm and a levee crest elevation of 41.15 cm.

Instrumentation and Analysis

As illustrated in Fig. 3, the instruments referenced in this paper and used in the data collection are of four major types: four floodwall wave gauges, four levee run-up gauges, nine overtopping containers, and five wireless wave gauges. The spacing of the gridlines in Fig. 3 is 1.52 m (5 ft) in model dimensions or 30.48 m (100 ft) in prototype dimensions. The floodwall gauges are located approximately 5–8 mm in front of the floodwall. Only three of the four gauges shown are used in the data analysis and results. The gauge

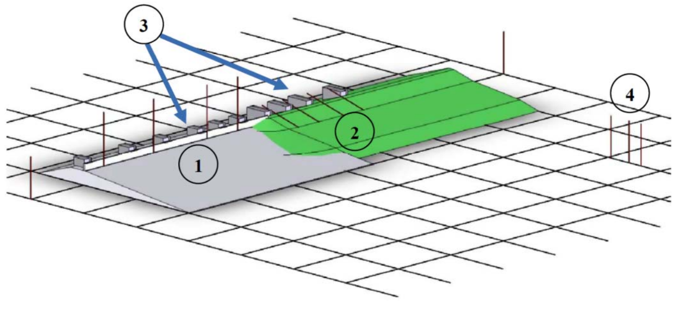

Fig. 3. Flood side of modeled levee transition and associated laboratory equipment: (1) floodwall wave gauges; (2) levee run-up gauges; (3) overtopping containers; (4) wireless capacitance three-gauge array

closest to the tank side wall was subject to model edge effects, notably refraction along the edge of the model, which resulted in unrealistic and inaccurate representations of the prototype structure; therefore, this gauge's data were omitted. From the three repeatability runs per each 10-min test, three statistical pieces of information are obtained from the three floodwall gauges' time series, each of which is determined from a zero upcrossing method of the time series: 2% floodwall crest elevation ($H_{2\%}$), floodwall significant wave height (H_s), and floodwall mean water level (MWL). From the zero upcrossing analysis, all wave heights recorded at the floodwall were ranked and the significant heights determined. The 2% floodwall crest elevation is defined as the floodwall crest elevation that is exceeded by only 2% of the incident waves, where the individual waves are likewise identified through an upcrossing analysis. The significant floodwall wave height is the average floodwall wave height of the highest one-third waves, whereas the floodwall MWL is defined as the average water level during the time series and is essentially the value of the SWL plus the wave-induced setup at the floodwall. Validation of the floodwall wave gauge measurements are based on visual observation and data analysis. Video and photography during the testing compared well with the measurements. From this video and data comparison, it can be stated that, in general, water splashing off the wall and hitting the wave gages was not registered as a high elevation by the instrument. However, any anomalous spikes in the time series were filtered, and repeatability runs provided consistent results.

Four run-up gauges are positioned along the upper levee section surface at a slope of 1V:4H. The gauges are positioned 1 mm away from the levee face to ensure the gauge does not remain wet as the water recedes down the levee's surface. Similar to the floodwall gauges, a zero upcrossing analysis of the gauges' time series enables calculation of the following statistics: 2% free surface elevation (2% η) and mean shoreline position (MSP). The 2% free surface elevation is defined as the surface elevation as measured by the gauge that is exceeded by only 2% of the incoming waves. This value is somewhat analogous to a run-up value, but because there is overtopping of the structure, any run-up value is ill-defined. The MSP is synonymous with the floodwall MWL and is the value of the SWL plus the wave-induced setup on the flood-side slope of the levee. Having multiple gauges along the structure allows the lateral variation of the measured values to be plotted, and use of MWL and MSP allows determination of the spatial variation of the wave-induced setup along the levee transition.

A total of nine overtopping containers are used in the data analysis and results. Just as the far-side floodwall gauge was subject to the refraction at the edge of the model, so is the overtopping container located at this location; therefore, the last overtopping container shown in Fig. 3 is omitted. The containers are fabricated from sheet metal and fit either directly on the floodwall or on the backside slope of the levee. Each is positioned and created so that the containers are immovable during testing and no water is capable of going under the container. The volume of water in the container, the time required to fill the container to the measured level, and the width of the opening of the are needed to determine the rate (l/s/m). This array of overtopping containers enables calculation of an overtopping distribution along the levee transition and allows correspondence of overtopping values to the measured wave heights and run-up values. As mentioned, the measured overtopping rates are directly compared with the empirical equations [Eqs. (1)–(4)]. In addition to the calculated values from the deterministic approach, values from a probabilistic approach (van Ledden et al. 2007) are provided. These values, based on a Monte-Carlo approach, are listed as q50 and q90 and are defined as the overtopping values exceeded by 50 and 10% of the storm events, respectively. In this analysis by van Ledden et al. (2007), storm wave and water level conditions are chosen randomly from a specified distribution, and thus these statistical exceedence values are representative of uncertainty in the hydrodynamic forcing. These empirical values are based on hydraulic conditions provided in Table 1.

Table 2. Prototype Hydraulic Conditions Achieved

Test No.	SWL (m)	H_{mo} (m)	T_p (S)
1	5.79	1.77	5.92
2	5.79	1.82	7.35
3	5.79	1.87	8.52
4	5.79	1.86	9.10
5	6.89	1.91	5.92
6	6.89	2.03	6.73
7	6.89	2.09	7.99
8	6.89	2.10	8.87

Three wave gauges are positioned in front of the levee section to create a three-gauge array for measurement of the incident wave heights created by the wave generator. This three-gauge array allows decomposition of the full wave spectrum into incident and reflected wave spectra by a least-squares method (Mansard and Funke 1980). The three-gauge array is located in the constant-depth portion of the tank away from the model, and can be interpreted as the wave height at the toe of the structure. Table 2 lists the hydraulic achieved conditions inside the wave basin. The hydraulic conditions achieved differ from the requested conditions, influenced mostly by wave-breaking energy loss very close to the wave maker, suggesting that the created waves are close to the steepest that can exist over a flat bottom.

Fig. 4 is a photograph of the levee transition model under testing at the Haynes Coastal Engineering Laboratory's shallow water wave basin. The wave parameters of Test No. 7 provide extreme floodwall wave heights and levee run-up values, which consequently yield significant overtopping rates along the entire levee transition. As a reminder, the floodwall crest elevation is 9.14 m in prototype dimensions.

Experimental Results

Levee Run-Up and Floodwall Wave Heights

Fig. 5 provides dimensional plots of two representative tests: No. 3 and No. 7. The top plots illustrate the floodwall wave heights and levee water elevations in prototype dimensions. The vertical datum

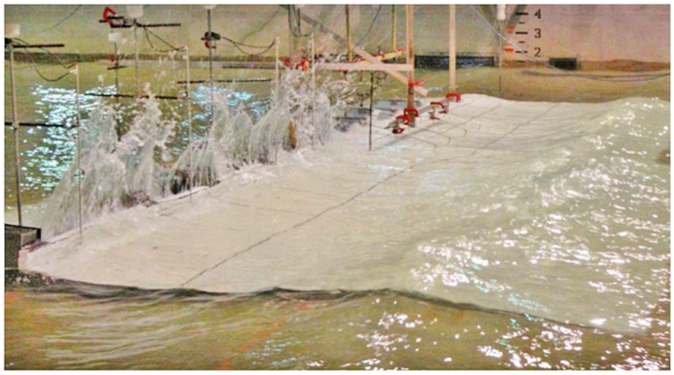

Fig. 4. Levee transition model during Test No. 7

for these statistical values is the toe of the levee, or the basin floor. The horizontal datum is the midpoint of the model, or at the transition between the two sections, where positive values are indicative of the levee section, and negative values represent the floodwall section. Each piece of statistical information from the floodwall wave gauges and levee run-up gauges is portrayed on the graphs. Each plotted value is the average of the repeatability runs for each test. In addition to this value, the total variation in results among the three runs is indicated by the error bar plots; however, in some results the precision among the three runs was very high, and it is difficult to see the error bars. There are many differences between the lower and higher SWL tests. As shown for Test No. 3, a recognizable feature of the floodwall wave heights is the gradual increase in the heights toward the transition during the lower SWL tests. The variations in floodwall wave heights and levee run-up values are directly influenced by the variations in MWL and MSP. As the wave-induced setup increases, so will the overall height of the depth-limited waves at the floodwall and the run-up values along the levee.

Essentially, the MWL and MSP are equivalent values and form a mean water level distribution across the entire model. As expected, the wave-induced setup is greater on a sloped structure, such as the levee section, than at a vertical wall. The variation in wave-induced setup ultimately influences the overall height of the floodwall wave heights and levee run-up. Because the MSP at the levee is greater than the MWL at the floodwall on the lower SWL tests, the MWL tends to increase toward the transition and levee section. This increase in MWL directly increases the floodwall wave heights (with respect to the toe of the levee) toward the transition as well. For the larger SWL tests, as shown for Test No. 7, the opposite is true for the variation in floodwall wave heights; instead, the values decrease toward the transition. Also noticeable is that the MWL is actually higher than the levee crest elevation and, therefore, larger than the MSP. This occurs because the floodwall crest elevation is greater than the levee crest elevation, which generates a flow around the floodwall crest at the transition, inducing a divergence at the transition. As a result, the MWL decreases toward the transition and so do the floodwall wave height values.

Overall, all wave height and run-up values are substantial, even for the lower SWL tests. For the majority of the tests, the floodwall wave crest elevations are well above the floodwall crest elevation, and 2% η is nearly equivalent to the levee crest elevation, indicating that a large fraction of waves are overtopping the structure. Of course, with an increase in the SWL, the run-up values and floodwall wave heights increase drastically, to 30 and 10%, respectively.

Overtopping Rates

The bottom subplots in Figs. 5(a) and 5(b) are comparisons of the measured overtopping rates and the empirically calculated overtopping rates based on Eqs. (1)–(4). The blue lines represent the averaged measured overtopping rates for the given test. The total range of values is again represented by the max/min bars at each measurement location. The floodwall side is indicated by the negative distance along the levee transition, and the levee section is indicated by the positive distance. As noted, the predictions from the deterministic equations [Eqs. (1)–(4)], as well as the probabilistic overtopping estimates, are provided to compare the measured results with expected, empirical results. The dashed black line represents the deterministic overtopping rate predicted from Eqs. (1)–(4). The green line is representative of the statistical q90 value, and the red dashed line is representative of the q50 value.

Immediately visible are the overtopping rates associated with the levee side of the protective structure. Clearly, the values of the levee side are much greater than those of the floodwall side. This is expected, and is consistent among all tests. Though the values may be much smaller on the floodwall side, according to the European overtopping manual (Pullen et al. 2007), discharges greater than 1.0 L/s/m can still induce erosion. For reference, discharges greater than 10 L/s/m will erode poorly protected levees and floodwalls; discharges greater than 50 L/s/m will result in damage to the crest and rear slopes, unless these areas are well protected.

There are considerable differences among the tests with different SWLs, especially in the overall magnitude of the results. The empirical equations predicted no overtopping along the floodwall for Test Nos. 1–3, which evidently is not the case as noted by the measured values. During the lower SWL tests, the floodwall section experienced overtopping rates ranging from 1 to 5 L/s/m. There is a gradual increase in the overtopping rates toward the transition along the floodwall, which is mimicked by the gradual increase in water level values along the floodwall. Also clearly shown are the underestimated overtopping rates on the levee side of the structure; this too is consistent for all tests. Only the q90 values from Test Nos. 1–3 provide a reasonable estimation of the measured overtopping rates on the levee side. For the lower SWL tests, the range of overtopping rates for the levee section range from approximately 10 L/s/m to more than 50 L/s/m, which could result in significant damage and erosion.

As predicted, the overtopping rates increased considerably for the higher SWL tests. The floodwall side experienced overtopping values ranging from approximately to nearly 175 L/s/m. The range is significant, and there is distinct variability along the floodwall, which is discussed further. For the levee side of the structure, tests beyond Test No. 3 yield measured overtopping rates well below the provided q90 value, concluding that the q90 value offers a conservative design approach for Test No. 4 and for the higher SWL tests, as shown in Fig. 5(b). For the floodwall side, tests beyond Test No. 6 also yield measured overtopping rates that are below the q90 value; therefore, the q90 value can also be considered conservative along the floodwall side for the extreme cases of Test Nos. 7 and 8. Overtopping rates for the high SWL tests would most likely exceed the design conditions for a well-protected structure. Again, the empirical overtopping rates calculated using Eqs. (1)–(4) tend to continually underestimate the measured values, and the estimate begins to converge closer to the q50 value on the levee side, indicating that the empirical overtopping equations are not well suited for calculation of the overtopping rates for this particular, spatially variable, protective structure.

J. Waterway, Port, Coastal, Ocean Eng. 2012.138:53-62.

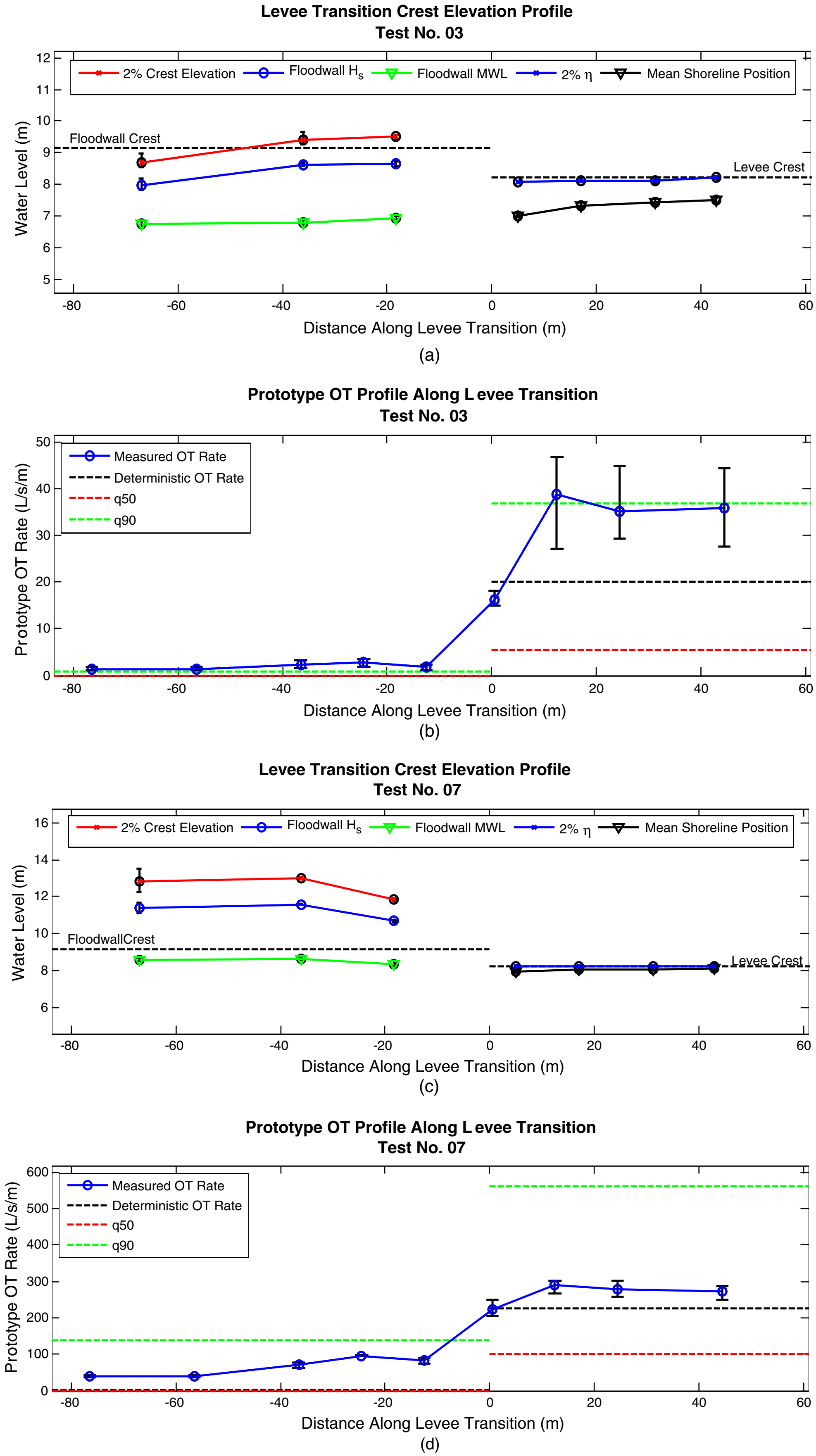

Fig. 5. Dimensional floodwall wave heights, levee water elevations, and overtopping (OT) rate distribution results from (a) Test No. 3 and (b) Test No. 7

J. Waterway, Port, Coastal, Ocean Eng. 2012.138:53-62.

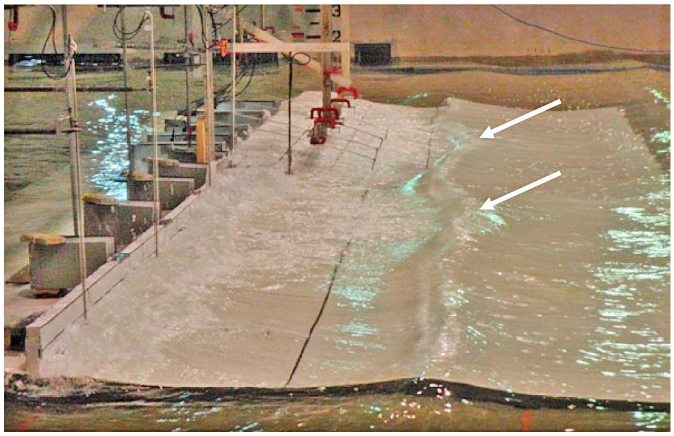

Fig. 6. Visual effects of undertow (highlighted by arrows)

In addition to the increase in SWL, the increase in peak period also directly increases overtopping rates; these results are mimicked by the general increase in floodwall wave heights and levee run-up values. One consistent trend in the spatial distribution of overtopping rates for all tests is the local overtopping peaks that occur at approximately −25 m on the floodwall side and at +15 to +30 m on the levee side. These results cannot be explained using empirical methods, which assume a uniform cross section along the length of a structure. In fact, these variations are generated from the three-dimensional contours at the transition, which in turn generate an undertow, as portrayed in Fig. 6.

At the transition, the contours cause the receding water to flow not only down the flood side of the structure, but also toward the floodwall side of the structure. As water flows down the contour in the longshore direction and down the structure in the cross-shore direction, a more prevalent undertow is generated near the −25-m region of the floodwall side. This undertow then causes the incident waves to refract. Also noticeable is the levee-side wave refraction, which occurs at approximately +20 m toward the levee. Because water is flowing down the contours away from the levee side, a divergence zone is created at the transition. As a result, water from the levee side attempts to fill this divergence; this flow, coupled with the receding water, causes this undertow and incident wave refraction evident at +20 m. In essence, there are two circulations, one rotating clockwise on the levee and another rotating counterclockwise over the transition region. Because of the wave refraction and current interaction, wave energy is focused at these locations, yielding higher overtopping values.

Dimensionless Floodwall Wave Heights and Levee Run-up

To analyze further the variable trends of the measured water level values and overtopping rates along the levee transition, as well as to compare these results with the empirical equations, a dimensionless analysis is conducted. To collapse the wave heights and water elevations experienced at the floodwall and the levee sections, these parameters are normalized by a combination of the incident characteristic wave height, H_i, the freeboard, R_c, and the SWL, h. A free parameter, ζ, is introduced as an exponent in the normalized values. To optimize the value of ζ, a MatLab® script is created to test a multitude of possibilities for the exponent's value. Ultimately, the script enables the user to define an array of values for ζ; it then applies this value to the dimensionless parameter and fits the resulting values with a least-squares fit. The ensuing coefficient of determination, or R^2 value, is then computed, and the most optimum value of ζ is chosen. In the following dimensionless parameters, the superscript t indicates a nondimensional parameter, and H_i is the measured incident characteristic wave height:

$$H^t_{2\%} = \frac{H_{2\%}}{H_i}\left(\frac{R_c}{h}\right) \tag{5}$$

$$H^t_s = \frac{H_s}{H_i}\left(\frac{R_c}{h}\right) \tag{6}$$

$$\mathrm{MWL}^t = \frac{\mathrm{MWL}}{H_i}\left(\frac{R_c}{h}\right) \tag{7}$$

$$2\%\eta^t = \frac{2\%\eta}{H_i}\left(\frac{R_c}{h}\right) \tag{8}$$

$$\mathrm{MSP}^t = \frac{\mathrm{MSP}}{H_i}\left(\frac{R_c}{h}\right)^{\zeta} \tag{9}$$

A dimensionless long-shore distance, x^l, is defined as

$$x^l = kx\Delta k = \frac{2\pi}{L_i} \tag{10}$$

where x = distance along the levee transition; the transition, or midpoint of the model, serves as the datum for the long-shore distance. The long-shore distance is normalized by the characteristic incident wavenumber, k, calculated at the three-gauge array, based on the peak spectral period at the structure toe water depth as measured by the incident wave gauges. The wavenumber is defined as the ratio in Eq. (10), where L_i is the characteristic incident wave length.

As noted, the floodwall wave heights differed as SWL increased. Not only did the magnitude of the wave heights increase, but the overall trend of the data differed. The wave heights tended to increase toward the transition for the lower SWL tests and decreased toward the transition for the higher SWL tests; thus, the exponent ζ is unnecessary and is omitted in Eqs. (5)–(7).

As representative plots of the gauge data at the floodwall and levee, the dimensionless floodwall MWL and levee MSP are plotted in Fig. 7. On each graph, all values from each test are plotted. As already noted, MSP and MWL are essentially equivalent and are a combination of SWL and the vertical rise in water level resulting from the wave-induced setup. Unlike the dimensional plots, innermost run-up and floodwall gauge are not coincident because of the difference in the dimensionless parameter. Immediately noticeable in Fig. 7(a) is the separation between the different SWL tests. The resulting dimensionless values tend to mimic the trends observed in the dimensional plots. In Fig. 7(b), however, there is not as much differentiation between the two SWLs, and the levee-side values tend to follow the same trend for both SWLs. In this case, the optimization variable ζ is used to obtain the most accurate collapse to obtain a R^2 value of approximately 0.60.

Dimensionless Overtopping Rates

Overtopping rates are normalized by methods outlined in the literature, and as before, the original ratio must be further scaled to alleviate the separation induced by the variation in water depth among the tests. The resulting dimensionless overtopping rate parameter is

$$q^t = \frac{Q}{\sqrt{gH_i^3}}\left(\frac{R_c}{h}\right)^{\zeta} \tag{11}$$

J. Waterway, Port, Coastal, Ocean Eng. 2012.138:53-62.

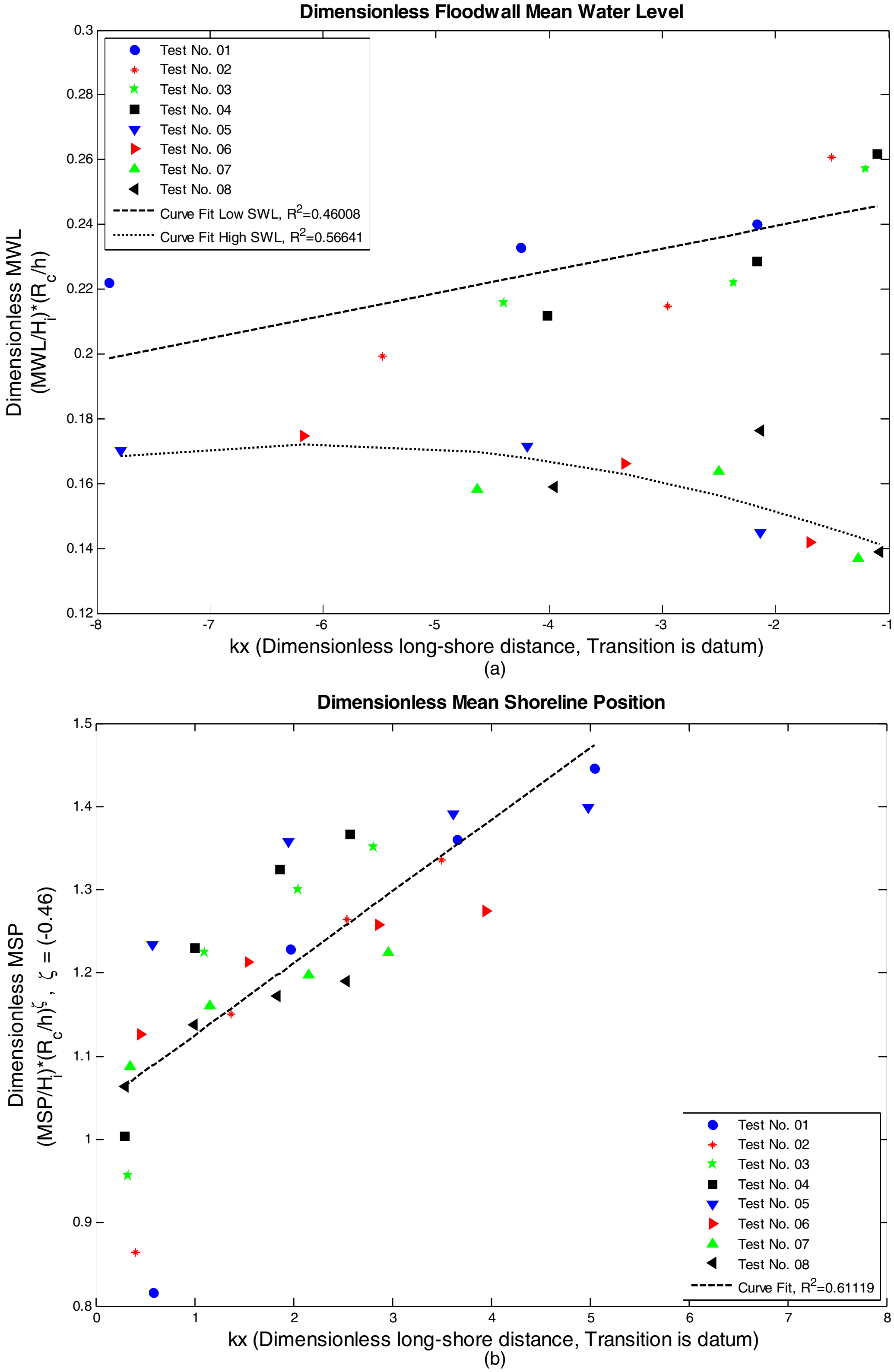

Fig. 7. Dimensionless water level value plots of (a) floodwall wave heights and (b) levee run-up

where Q represents the measured overtopping rate, the superscript t denotes the nondimensionality, and the exponent ζ provides the means of optimizing the ratio, generating the most efficient collapse of the data, as already detailed.

The resulting plots of the dimensionless overtopping rates are displayed in Fig. 8. Because of the significantly different overtopping rates experienced at the floodwall section compared with the levee section, the two sections are independently analyzed. Fig. 8(a) depicts the floodwall overtopping rates. The value of ζ is iteratively calculated to be 4.415, yielding an R^2 value of nearly 0.40. The quadratic least-squares fit provides the general fit to the data, expressing an overall increase in the dimensionless parameter toward the transition, conveying that the overtopping generally increases toward the transition. Fig. 8(b) provides the results of the dimensionless overtopping rates on the levee side. These values did not collapse as well as the floodwall overtopping rates, but they did maintain the overall parabolic trend. With a ζ equaling 2.81 and an R^2 value of only 0.18, the plot suggests a parabolic tendency along the levee section, denoting that the maximum overtopping generally occurs around $kx = 2$.

It is reasonable to state that the dimensionless analysis does not provide enough conclusive evidence to generate a confident expression relating the hydraulic and geometric parameters of the test to the overtopping rates experienced along the levee transition

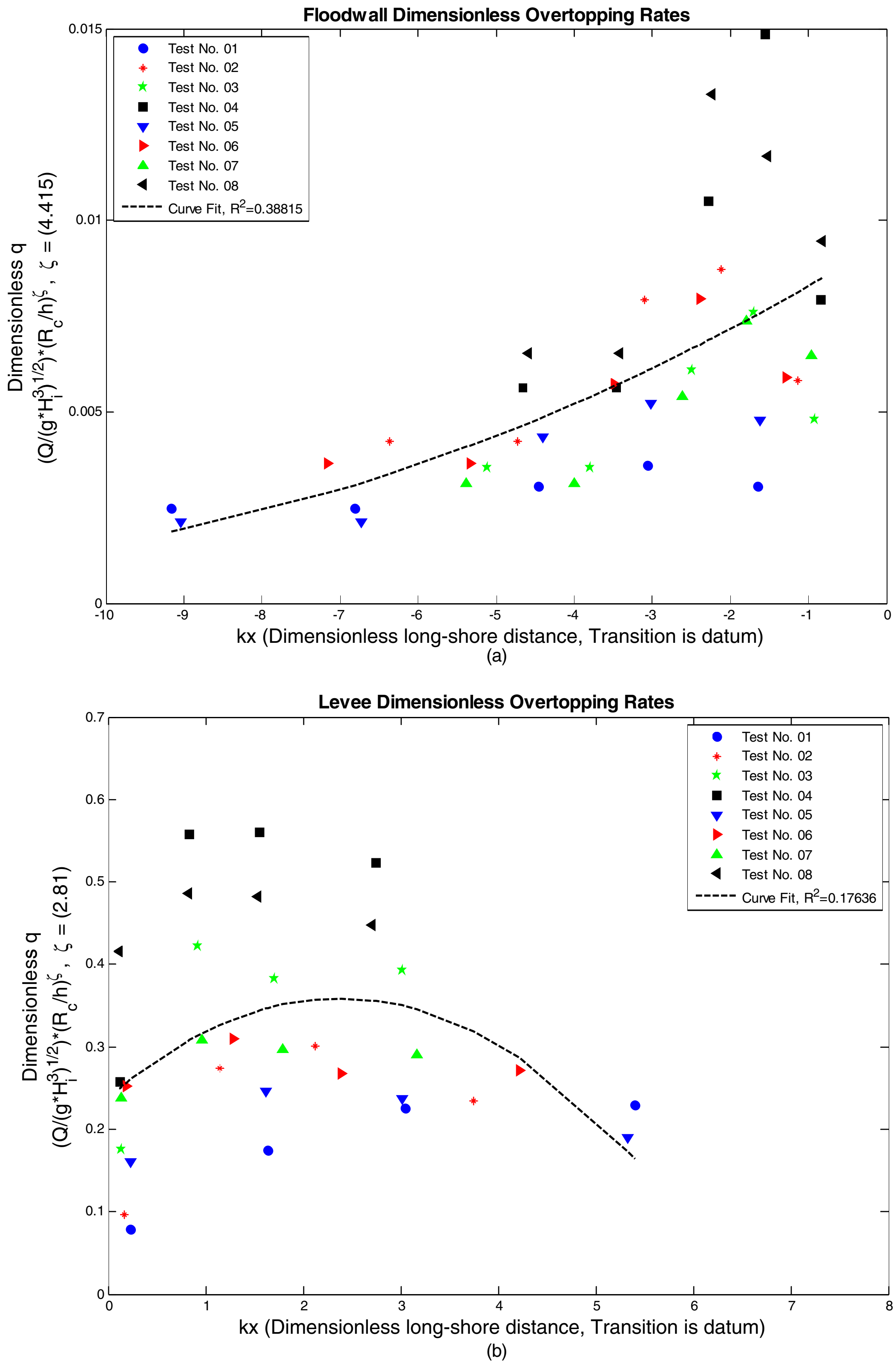

Fig. 8. Dimensionless overtopping rates at (a) floodwall and (b) levee sections

J. Waterway, Port, Coastal, Ocean Eng. 2012.138:53-62.

structure. There is extreme variability along the levee transition, and the generic nondimensional methodologies are not applicable to such a nonlinear and three-dimensional evaluation. However, for engineering problems these results can at least provide approximate guidance for a problem where there is little.

Summary and Conclusions

The research presented here outlines the evaluation and assessment of a specific levee transition structure tested under extreme design conditions. Tests varied hydraulic conditions such as incident wave period, incident wave height, and still water level. Response of the structure was investigated within a three-dimensional shallow water wave basin stationed within the Reta and Bill Haynes'46 Coastal Engineering Laboratory at Texas A&M University, College Station, Texas. The results of the testing were analyzed both dimensionally and nondimensionally to help present the mechanisms contributing to the measured floodwall wave heights, levee run-up, and overtopping rate distribution along the levee transition structure. From the results, there is evidence that the methodologies employed to estimate the overtopping rates on the levee transition underestimate the measured values. The observed trends indicate spatial variability among the measured values along the levee transition caused by inherent three-dimensional effects, such as observed undertow generated by the levee transition contours, which would otherwise be unnoticed without three-dimensional physical modeling. For the tests undertaken at the laboratory, the most influential parameter for the overtopping rates and water levels measured at the structure was the variation in the SWL. Longer peak periods also resulted in higher overtopping rates and water level values at the structure. Measured overtopping rates exceeded 300 $L/s/m$ on the levee section of the structure and 100 $L/s/m$ on the floodwall section for the extreme hydraulic conditions, all of which were underestimated by existing empirical methods. Floodwall wave crest elevations were measured up to 4–5 m above the floodwall crest elevation, and wave-induced setups allowed mean water levels to essentially equal the height of the structure. Overall, the measured values were substantial, and would ultimately require the structure to be well protected against the erosion effects induced by the hydraulic conditions.

References

Hughes, S. A. (2008). "Levee overtopping design guidance: What we know and what we need." *Proc., Solutions Coastal Disasters Congr.*, Vol. 78, L. Wallendorf, L. Ewing, C. Jones and B. Jaffe, eds., ASCE, New York, 867–877.

Hughes, S. A., and Nadal, N. C. (2008). "Laboratory study of combined wave overtopping and storm surge overflow of a levee." *Coast. Eng.*, 56(3), 244–259.

Link, L. E. (2010). "The anatomy of a disaster, an overview of Hurricane Katrina and New Orleans." *Ocean Eng.*, 37(1), 4–12.

Mansard, E. P. D., and Funke, E. R. (1980). "The measurement of incident and reflected spectra using a least squares method." *Proc., 17th Int. Coast. Eng. Conf.*, Vol. 2, ASCE, New York, 154–172.

Nicholson, P. G. (2007). "Preliminary reconnaissance and observations of the New Orleans levee and floodwall failures by independent assessment teams." *Proc. Geo-Denver 2007: New Peaks Geotechnics Conf., Geotechnical Specialty Publications: Embankments, Dams, and Slopes*, Vol. 13, ASCE, New York, 224–233.

Pullen, T., Allsop, N. W. H., Burce, T., Kortenhaus, A., Schüttrumpf, H., and van der Meer, J. W. (2007). "EurOtop: Wave overtopping of sea defences and related structures: Assessment manual." ⟨www.overtopping-manual.com⟩.

Schüttrumpf, H., and van Gent, M. R. A. (2003). "Wave overtopping at seadikes." *Proc. Coast. Struct. Conf.*, ASCE, New York, 431–443.

Sills, G. L., Vroman, N. D., Wahl, R. E., and Schwanz, N. T. (2008). "Overview of New Orleans levee failures: Lessons learned and their impact on national levee design and assessment." *J. Geotech. Geoenviron. Eng.*, 134(5), 556–565.

Technical Advisory Committee for Flood Defence in the Netherlands (TAW). (2002). "Wave run-up and wave overtopping at dikes." *Technical Report compiled at the request of the Road & Hydraulic Engineering Institute under the auspices of TAW*, TAW, Delft.

Van der Meer, J. W., and Janssen, W. (1995). "Wave run-up and wave overtopping at dikes." *Wave Forces on Inclined and Vertical Wall Structures*, N. Kobayashi and Z. Demirbilek, eds., ASCE, New York, 1–27.

Van Ledden, M., Lynett, P., Resio, D. T., and Powell, N. J. (2007). "Probabilistic design method of levee and floodwall heights for the hurricane protection system in the New Orleans area." *Proc. 10th Int. Workshop Wave Hindcasting Forecasting Coastal Hazard Symposium.* JCOMM, available online at: ⟨http://www.waveworkshop.org/10thWaves/Papers/VanLeddenetal_Hawaii_2007.PDF⟩.